Published in final edited form as:
Free Radic Biol Med. 2009 October 1; 47(7): 962–968. doi:10.1016/j.freeradbiomed.2009.06.031.

DECREASED S-NITROSATION OF PEPTIDE THIOLS IN THE MEMBRANE INTERIOR

Hao Zhang[1], **Christopher Andrekopoulos**[2], **Yingkai Xu**[3], **Joy Joseph**, **Neil Hogg**, **Jimmy Feix**, and **B. Kalyanaraman**[*]
Department of Biophysics, Medical College of Wisconsin, Milwaukee, WI USA

Abstract

It has been proposed that autoxidation of nitric oxide (˙NO) stimulates S-nitrosation of thiols located in the hydrophobic milieu. We tested whether thiols located in hydrophobic membranes undergo enhanced S-nitrosation in the presence of ˙NO/O_2. Transmembrane cysteinyl peptides, C_4 (AcNH-KKA**C**ALA(LA)$_6$KK-CONH$_2$); C_8 (AcNH-KKALALA**C**ALA(LA)$_3$KK-CONH$_2$), were incorporated into dilauroylphosphatidylcholine (DLPC) bilayers; their location in the membrane was determined by EPR spin labeling. The peptides, C_8 and C_4, and GSH (300 μM) were treated with a ˙NO donor, DEA-NONOate, and nitrosothiol formation determined under different O_2 levels. Surprisingly, the more hydrophobic cysteinyl peptide, C_8, did not yield any S-nitrosated product compared to GSH in the aqueous phase or C_4 peptide in the liposomes in the presence of ˙NO/O_2. This data suggests that thiols located deeply in the hydrophobic core of the membrane may be less likely to undergo S-nitrosation in the presence of ˙NO/O_2.

Keywords

S-nitrosation; spin labeling; membrane; diffusion and reactions of nitric oxide; model membrane

INTRODUCTION

Increasing evidence suggests that S-nitrosation of protein thiols is a key post-translational modification that has a profound effect on protein function, redox signaling, and signal transduction mechanisms [1-3]. The list of key physiologically relevant enzymes that can potentially be regulated by S-nitrosation is steadily growing [2,4-7]. The mechanism of S-nitrosation of protein thiols under *in vivo* conditions is still under investigation. Reports indicate that autoxidation of ˙NO stimulates S-nitrosation reactions. In this reaction, ˙NO and molecular oxygen form nitrogen di-oxide (˙NO_2), which may react with thiol to form a thiyl radical that rapidly combines with ˙NO to form an S-nitrosothiol. Alternatively, ˙NO_2 may react with ˙NO to form dinitrogen trioxide (N_2O_3) which may nitrosate the sulfhydryl group [8-10]. However, the biological significance of these reaction mechanisms had been questioned because the rate-

[*]**Correspondence should be addressed to:** Dr. B. Kalyanaraman, Department of Biophysics, Medical College of Wisconsin, 8701 Watertown Plank Road, P.O. Box 26509, Milwaukee, WI 53226 USA; Tel: 414-456-4000; Fax: 414-456-6512; balarama@mcw.edu.
[1]Current address: Department of Surgery, Medical College of Wisconsin, Milwaukee, WI
[2]Current address: 2815 W. Lunt Ave. #2, Chicago, IL 60645
[3]Current address: EPR Core Lab, Dorothy M. Davis Heart and Lung Research Institute, Ohio State University, Columbus, OH

limiting step is a second order in ·NO and first order with respect to O_2. At physiological ·NO and O_2 levels, it is kinetically unfavorable [11]. However, their relative concentrations in hydrophobic membranes are much higher, as both molecular O_2 and ·NO are lipophilic [12, 13]. Consequently, the rate of formation of N_2O_3 was estimated to be at least 300-fold higher in hydrophobic membranes as compared to the aqueous phase [14,15]. This has lead to the speculation that thiol groups present within, or in close proximity to, membranes or hydrophobic protein domains are more prone to undergo S-nitrosation *via* this mechanism [16]. However, this reaction (i.e., S-nitrosation of hydrophobic thiols in the presence of ·NO/O_2) has never been tested experimentally in a well-defined model system. To investigate whether thiols located in hydrophobic membranes undergo enhanced S-nitrosation, we designed a model membrane system in which transmembrane cysteinyl peptides with cysteine located at different positions were incorporated into saturated DLPC liposomes. The present data show that thiols located in more hydrophobic regions undergo less S-nitrosation in the presence of ·NO and O_2 as compared to thiols located in more hydrophilic environments.

MATERIALS AND METHODS

Peptide synthesis and purification

Transmembrane peptides had acetylated N-termini and amide-blocked C-termini. Peptides were chemically synthesized using the standard Fmoc solid phase peptide synthesis chemistry and an Advanced Chemtech (Louisville, KY) Model 90 synthesizer and purified by semipreparative reverse phase HPLC and molecular weight determined by LC-MS as described previously [17].

Synthesis, purification, and detection of S-nitrosopeptides

The C_4 or C_8 peptides (1 mM) were treated with S-nitrosoglutathione (GSNO) (20 mM) in a 50% methanol and 50% phosphate buffer (50 mM, pH 7.4) mixture containing DTPA (100 μM) at room temperature for 15 min. GSNO was prepared according to published methods [18]. The concentration of the S-nitrosated peptide was determined using the Saville's reaction [19]. ^{15}N-labeled C_4-SNO was prepared by treating C_4 with ^{15}N-labeled GSNO. After separating by HPLC, mass spectral studies on ^{14} N- and ^{15}N-labeled nitrosothiols were carried out (Fig. S2 in Supplementary Information).

Incorporation of pure and spin labeled C_4 and C_8 peptides into liposomes

Liposomes were prepared according to published methods [20]. A methonolic solution of the peptide was added to DLPC in methanol. The mixture was dried under a stream of N_2 gas and kept in a vacuum dessicator overnight. Multilamellar liposomes were prepared by thoroughly mixing the dried lipid in phosphate buffer (100 mM, pH 7.4) containing DTPA (100 μM). Unilamellar liposomes were prepared by freeze-thawing (5 cycles) in liquid nitrogen, followed by 25 cycles of extrusion through a 0.2 um polycarbonate filter (Nucleopore, Pleasanton, CA) in an extrusion apparatus (Lipex Biomembranes Inc., Vancouver, BC).

The C_4 or C_8 peptide was mixed with methanethiosulfonate (MTSL) (5 mM) in a 50% methanol and distilled water solution at 4°C overnight (Fig. S3 in Supplementary Information). The spin labeled peptide was separated on a HPLC system and lyophilized. The spin labeled C_4 and C_8 peptide was incorporated into liposomes as described above, while ensuring that the ratio of peptide to lipid was 1:500. Spin labeled peptides incorporated liposomes were then concentrated by ultracentrifugation. A similar procedure was followed for blocking reactive thiols with methyl methanethiosulfonate (MMTS).

HPLC analyses of nitrosated peptides

Briefly, a 20 μl of sample was injected into a HPLC system (HP1100) with a C-18 column (250×2 mm) equilibrated with 0.1% trifluoroacetic acid. The parent peptides and the S-nitrosated peptides were separated by a linear increase of acetonitrile concentration (1% per min) at a flow rate of 0.2 ml/min. S-nitrosated peptides were detected using a variable detector at 336 nm.

Tri-iodide detection of S-nitrosated peptides: Detection levels

The DLPC liposomes containing the transmembrane peptide, after incubation with DEA-NONOate at 37°C, were dissolved in methanol (1:1, v/v) and free thiols were blocked by trating with iodoacetamide for 30 min. Free nitrite in these samples were scavenged by adding 10% (v/v) of ammonium sulfamide (20%) in 2N HCl at room temperature for 15 min (Fig. S4 in Supplementary Information). Where indicated, $HgCl_2$ (5 mM) was added immediately after adding ammonium sulfamide. Formation of S-nitrosated thiols were detected in a Sievers Model 280A ·NO analyzer by ozone-based chemiluminescence. Typically, samples (20-300 μl) were injected into a purge vessel containing a 5 ml reaction mixture (5.6 mg/ml of KI and 3.6 mg/ml of iodine in 13.6 M acetic acid. The amount of S-nitrosothiol was quantitated by comparing the signal with those obtained from an authentic nitrosothiol. Under these experimental conditions, the linear detection range was from 5 pmol to 400 pmol. The detection limit was 2 pmol (i.e., 10 nM using a 300 μl injection volume).

Electron paramagnetic resonance (EPR) methods: Microwave power saturation

EPR spectroscopy was performed on a Varian E-102 Century series X-band spectrometer equipped with a loop-gap resonator. Samples were run in a gas-permeable TPX capillary. Spectra were recorded using 1 mW incident microwave power and a modulation amplitude of 1 G. Microwave power saturation experiments were carried out using varying microwave powers (0.1-50 mW). Samples in the TPX capillary were purged with a continuous stream of air (20% oxygen) or nitrogen or in the presence of NiEDDA under nitrogen. The peak-to-peak intensity of the center line (M_i=0) of the EPR spectra were plotted against the square root of the incident microwave power.

RESULTS

Location of transmembrane cysteinyl peptides

We synthesized and purified the cysteinyl peptides, C_4 (AcNH-KKA**C**ALALALALALALALAKK-$CONH_2$) and C_8 (AcNH-KKALALA**C**ALALALALALALAKK-$CONH_2$). These peptides were subsequently incorporated into dilauroylphosphatidylcholine (DLPC) liposomes containing saturated alkyl chains. The position at which the cysteinyl residue was located in the membrane was determined by EPR spin labeling methodology [21]. Each peptide was treated with the sulfydryl-specific nitroxide spin label, MTSL (Fig. S1 in Supplementary Information). Figure 1 shows the EPR spectrum of MTSL-labeled C_4 peptide. The EPR spectrum is homogeneous and motionally restricted, consisting of a single component. The location of the nitroxide attached to a specific cysteinyl residue in the bilayer was determined by continuous wave power saturation EPR measurements in the presence of oxygen, nitrogen, and the polar paramagnetic agent, nickel (II) ethylenediaminediacetate (NiEDDA) [22,23]. Typically, under nonsaturating conditions, the height of the spectral line is proportional to the incident microwave power and increases linearly with the square-root of the incident power, $P_{1/2}$. At higher microwave powers, the signal intensity begins to decrease due to power saturation. In the presence of a paramagnetic relaxation agent that interacts with the nitroxide through a bimolecular collision mechanism, the relaxation rate is enhanced; this allows the sample to absorb more microwave

power prior to saturation [21]. The concentration of molecular oxygen, a small hydrophobic paramagnetic molecule, is increased in the center of the lipid bilayers. In contrast, NiEDDA, a neutral, water-soluble paramagnetic agent, concentrates mainly in the aqueous phase and not in the center of the lipid bilayers. The relative extent of the interaction between the spin-labeled peptide and these two paramagnetic agents gives valuable information concerning the molecular location of the spin-labeled cysteinyl peptide [22,23]. Based on comparison with lipid spin label standards, the position of the nitroxide attached to the C_4 and C_8 cysteinyl thiols was estimated to be at a depth of 9 ± 1 Å and 12.5 ± 1 Å below the lipid phosphates, respectively.

HPLC analysis of S-nitrosation of transmembrane hydrophobic thiols (C_4 and C_8) and glutathione induced by ·NO and O_2

Authentic S-nitrosated standards of C_4 and C_8 peptides (C_4-SNO and C_8-SNO) were prepared *via* transnitrosation reaction between GSNO and C_4 and C_8. After purification using a preparative HPLC method, molecular weights of the nitrosated products were determined by ESI-MS. As shown in Figure 2a-c (*top trace*), the authentic standards C_8-SNO (4 μM), C_4-SNO (20 μM), and GSNO (20 μM) were separated and detected by HPLC-UV at 336 nm. The HPLC-MS results were further confirmed using the ^{15}N-labeled nitrosated products (e.g., C_4-S^{15}NO) (Fig. S2 in Supplementary Information). To investigate ·NO/O_2-mediated nitrosation of thiols, C_4 and C_8 in liposomes and GSH in a phosphate buffer containing DTPA (100 μM) were incubated with DEA-NONOate, a ·NO donor that spontaneously releases ·NO [$t_{1/2}$=16 min in phosphate buffer (pH 7.4) at 37°C] for 20 min [24,25]. After blocking the unreacted thiols with iodoacetamide (50 mM), reaction mixtures were separated and detected by HPLC at 210 nm and 336 nm. Figure 2a-c (*middle trace*) shows the HPLC profiles of S-nitrosated products formed from C_8 and C_4 peptides, and GSH incubated with DEA-NONOate. Surprisingly, C_8-SNO was not detectable under these conditions. The increase in C_4-SNO formation was modest compared to GSNO formation. Figure 2a-c (*bottom trace*) shows the HPLC profiles in the absence of DEA-NONOate. Figure 3a shows the yields of nitrosothiols formed from incubating C_4 or C_8 (300 μM) in DLPC liposome (30 mM) or GSH (300 μM) in phosphate buffer in the presence of varying concentrations of DEA-NONOate (0-500 μM). Both GSNO and C_4-SNO increased linearly up to 250 μM of DEA-NONOate, although the yields of GSNO were 2- to 3-fold higher over this range (0-250 μM). At much higher concentrations of DEA-NONOate (500 μM), the C_4-SNO levels slightly decreased, the reasons for which are not clear at present. Again, the most intriguing finding is that the C_8-SNO levels were barely detectable over a wide range of DEANONOate concentrations (0-500 μM), although there was a decrease in C_8 peptide levels (Fig. 3b), indicating that ·NO or oxidants derived from it reacted with C_8 thiols in the hydrophobic environment. These results suggest that a decrease in the hydrophobicity will stimulate ·NO/O_2-mediated S-nitrosation of transmembrane cysteinyl peptides.

Tri-iodide chemiluminescence analyses of S-nitrosation of C_4, C_8, and GSH induced by ·NO and O_2

Further validation of HPLC results was obtained using a highly sensitive tri-iodide chemiluminescence method capable of detecting 1-2 picomoles of S-nitrosated thiols [26,27]. Establishing a standard curve for authentic GSNO, C_4-SNO, and C_8-SNO was essential to rule out the structural dependency of signals obtained from the Siever's analyzer. As shown in Figures 4a and b, similar traces were obtained from the ·NO analyzer in response to injecting GSNO and C_8-SNO (5-20 pmol). The addition of mercuric chloride ($HgCl_2$) totally abrogated the chemiluminescence signal obtained from 20 pmoles of GSNO or C_8-SNO, indicating that nitrosothiols are responsible for chemiluminescence signals. As autoxidation of ·NO generates large amounts of nitrite, we determined the optimal quantity of ammonium sulfamide (a nitrite scavenger) to be included in subsequent experiments in order to eliminate nitrite-mediated artifacts. Figure 4c shows the actual traces obtained from the ·NO analyzer after injecting 200

pmol of nitrite in the presence of different concentrations of ammonium sulfamide. Results indicate that 1% of ammonium sulfamide (final concentration) was sufficient to scavenge all nitrite. Finally, we determined whether DLPC liposome interfered with hydrophobic membrane nitrosothiol detection. Figure 4d shows the traces obtained after injecting C_8-SNO (5 pmoles) and C_8-SNO (5 pmoles) in DLPC liposome (30 mM lipid) into the ·NO analyzer, indicating no interference from liposomes on chemiluminescence signals obtained from nitrosothiol.

Next we investigated nitrosothiol formation, using the tri-iodide chemiluminescence method, during the reaction between ·NO/O_2 and C_4, C_8, and GSH. Incubation conditions were identical to those described for HPLC analyses. Figure 5 (*left panel*) shows the chemiluminescence signal obtained upon injecting 10 μL sample of an incubation mixture containing GSH (300 μM) and DEA-NONOate in aerobic phosphate buffer. This signal represents 19 ± 4 μM (n=4). Figure 5 (*middle panel*) represents the chemiluminescence signal formed from injecting a sample from incubations containing C_4 incorporated into DLPC, and DEA-NONOate. The injection volume was 5-fold higher than the GSH reaction mixture. In the presence of $HgCl_2$ no signals were detected. Again, we could not detect any signal from the reaction between C_8 and DEA-NONOate under otherwise similar incubating conditions (Fig. 5, *right panel*). Even with 30 times the injection volume used in GSH experiment, no signal was detected from the C_8 reaction with DEA-NONOate (Fig. 5, *right panel*). Thus, on the basis of results obtained from using two different approaches, we conclude that S-nitrosation of thiols located in hydrophobic membranes is dramatically inhibited during ·NO autoxidation.

We then investigated the oxygen dependency on nitrosothiol formation, because of a bell-shaped response reported previously for S-nitrosation of thiols in aqueous solution [10]. We surmised that a plausible reason for the lack of S-nitrosation of C_8 peptide in DLPC membrane could be due to the higher oxygen concentration in the most hydrophobic region of the membrane. Figure 6a shows the influence of 100% air and argon on ·NO-dependent nitrosation of GSH in phosphate buffer. Next, we compared the levels of GSNO, C_4-SNO, and C_8-SNO as a function of air concentration in incubations containing GSH, C_4, C_8 and DEA-NONOate performed in a glove box. We observed a bell shaped response with respect to GSNO and C_4-SNO formation with a maximum S-nitrosation yield occurring at 30 μM oxygen (15% air). Compared to GSH and C_4, the nitrosation of C_8 peptide was negligible at various aerobic concentrations (Fig. 6b, *bottom trace*). These results strongly suggest that the lack of S-nitrosation of C_8 is not due to the higher concentration of oxygen in the more hydrophobic region of DLPC membrane.

Modification of thiols in C_4-SH peptide with MMTS, a thiol modifying agent, totally inhibited formation of C_4-SNO during incubation C_4 peptide with various concentrations of nitric oxide donor (Fig. S3 in Supplementary Information).

DISCUSSION

It is well established that N_2O_3, formed during ·NO reaction with O_2, reacts with thiolate anions to form nitrosothiols [9]. It was proposed that N_2O_3-dependent S-nitrosation is highly efficient and focused by hydrophobic membranes [14,15]. The prevailing view is that the local hydrophobicity might promote S-nitrosation of cysteine thiols in the hydrophobic membrane [28,29]. S-nitrosothiols are typically formed *via* donation of a nitrosonium ion (NO^+) from N_2O_3 to the nucleophilic thiolate anion ($RS^- + NO^+ \rightarrow RSNO$). Thus, this reaction is unlikely to occur in the hydrophobic regions of the membranes where cysteinyl thiols remain protonated. Consistent with this prediction, addition of DEA-NONOate (up to 500 μM) to DLPC membranes incorporated with 100 μM C_8 peptide did not induce S-nitrosation. Hydrophobicity in the membrane is largely governed by the extent of water penetration [30]. A typical

hydrophobicity profile across saturated membranes is shown in Figure 7. The local hydrophobicity was determined by measuring the Z component of the hyperfine tensor (A_z) of the nitroxide spin probe incorporated at different depths in the membrane. Based on these measurements, the water concentration near the hydrophobic center of the bilayers is estimated to be approximately 50 mM, or about 0.1% of that in the bulk aqueous phase. A decrease in the membrane hydrophobicity (i.e., increase in water penetration into the membranes) will stimulate $^{\cdot}NO/O_2$-mediated S-nitrosation of transmembrane cysteinyl peptides as shown in Figure 7.

To characterize the accessibility of transmembrane thiols to the aqueous phase, the microwave power saturation technique in the presence of air, nitrogen, or paramagnetic NiEDDA has previously been used [21-23]. If the spin labeled nitroxide is in an aqueous environment, it takes a much higher microwave power to saturate the signal in the presence of water-soluble NiEDDA than in the presence of oxygen. Alternatively, if the nitroxide were to be located in the interior of the bilayer, the opposite would be true (i.e., higher microwave power needed to saturate in the presence of oxygen than in the presence of NiEDDA). The change in the half-saturation parameter, $\Delta P_{1/2}$, derived from the continuous wave (CW) power saturation graphs (Fig. 1) directly measures the bimolecular collision rate between the nitroxide and the paramagnetic relaxation agent (oxygen or NiEDDA). Thus, accessibility to NiEDDA is given by:

$$\Delta P_{1/2}\,(\mathrm{NiEDDA}) = P_{1/2}\,(\mathrm{NiEDDA}) - P_{1/2}\,(\mathrm{N_2})$$

and a similar relationship defines accessibility to O_2.

Relative accessibilities to O_2 and NiEDDA are given by the EPR depth parameter, Ø:

$$\varnothing = 1\mathrm{n}\left[\frac{\Delta P_{1/2}\,(\mathrm{O_2})}{\Delta P_{1/2}\,(\mathrm{NiEDDA})}\right]$$

The Phi value Ø is proportional to membrane depth [22,23], and is expected to correlate with the accessibility of the spin labeled thiol group to nitrosating agents. Our data show that C_8 does not undergo S-nitrosation as compared to C_4. The Phi values for C_4 peptide and C_8 peptide were measured to be approximately 1.85 and 2.2. Phi values have a standard deviation of ± 0.1, so that the calculated depths of spin labels at C4 and C8 are 8.2 (± 0.8) Å and 10.5 (± 0.9) Å, respectively. However, it has been noted that there is a sharp transition in the hydrophobicity profile of the membrane, with polarity decreasing significantly over the distance of a single C-C bond [31]. Consequently, even this relatively small distance separation can result in marked differences in local polarity. It would appear that there is sufficient water penetration so that the C_4 thiols are partially ionized, making it kinetically possible to react with nitrosating agent (N_2O_3 or NOX) formed from $^{\cdot}NO$ and O_2. In the DLPC membranes, the C_8 thiols are probably not ionized, thus restricting the reaction between the C_8 –SH group and NOx or N_2O_3. These results suggest that the accessibility parameter may be used as a predictor of whether a particular thiol is more or less susceptible to undergo S-nitrosation in the presence of $^{\cdot}NO$ and O_2.

It has been suggested that the presence of nearby amino acids capable of altering the cysteine protonation state may play an important role in mediating Cys nitrosation [32,33]. However, the ability of a nearby amino acid to influence cysteine protonation generally requires a well-defined structural association between the two amino acids, which probably does not occur in these flexible peptides. In addition, the lysine residues in these peptides are located in the

aqueous phase above the plane of the membrane where they are most likely to interact with water, whereas the cysteine residues are clearly buried in the hydrophobic phase of the bilayer. Thus, the role of lysine residues on cys deprotonation in the present case appears to be tenuous. Nonetheless, we cannot completely rule out the possibility that the smaller separation between C4 and the N-terminal lysine residues plays a role in enhancing nitrosation at the C4 position. Additional model peptides with lysine incorporated in the middle of the membrane need to be carefully designed with appropriate controls.

Nitric oxide-dependent posttranslational modifications (nitrosation and oxidation of peptidyl cysteine residues and protein tyrosyl nitration) have heen detected in human diseases [34,35]. In principle, all thiols are susceptible to S-nitrosation. However, it is evident from these studies that this nitrosative modification is selective for specific cysteines [32]. Recent reports suggest that intramolecular electron transfer mechanism govern the selectivity of Cys oxidation and nitrosation [36]. The present results indicate that cysteinyl thiols located in the hydrophobic core of the membrane bilayer in DLPC bialyers do not undergo S-nitrosation reactions in the presence of $^{\cdot}NO$ and O_2. Although it would be desirable to perform these experiments at much lower concentrations of $^{\cdot}NO$ (that closely mimics physiological conditions) where the catalytic effect of the membrane is more pronounced, we do not have access to more sensitive technology that will reliably detect such a low level of nitrosation.

Based on the diffusion and reactivity characteristics of $^{\cdot}NO$, it was also suggested that cysteinyl residues located in hydrophobic regions within a protein are unlikely targets for S-nitrosation [37]. Although the hydrophobic cysteines (with low solvent accessibility) present in the protein sarco/endoplasmic reticulum Ca-ATPase (SERCA) undergo efficient oxidation under nitrosative and nitrative stress, a tyrosyl radical-mediated electron-transfer mechanism has been proposed in these systems [38].

SUMMARY/CONCLUSION

Transmembrane profiles of the O_2 diffusion-concentration product have been determined in a variety of model membrane systems composed of both saturated and unsaturated lipids, in the presence and absence of cholesterol, with and without integral membrane proteins [31]. In all cases these profiles have a similar bell-shaped dependence on membrane depth, with high O_2 levels near the center of the bilayer, and the transmembrane profile of $^{\cdot}NO$ has been shown to be quite similar [20]. Transmembrane profiles of water penetration have a comparable bell-shaped dependence on membrane depth, but with decreasing water concentration near the center of the bilayer [31]. The consistency of these profiles across many different membrane compositions strongly suggests that a similar dependence will exist in native biological membranes.

Supplementary Material

Refer to Web version on PubMed Central for supplementary material.

Acknowledgments

This work was supported by National Institutes of Health Grant HL063119.

LIST OF ABBREVIATIONS

CW	continuous wave
DLPC	dilauroylphosphatidylcholine

GSNO	S-Nitrosoglutathione
($HgCl_2$)	mercuric chloride
$^{\cdot}NO$	nitric oxide
N_2O_3	dinitrogen trioxide
$^{\cdot}NO_2$	nitrogen di-oxide
MMTS	methyl methanethiosulfonate
NiEDDA	nickel (II) ethylenediaminediacetate
MTSL	methanethiosulfonate
SERCA	sarco/endoplasmic reticulum Ca-ATPase

REFERENCES

1. Hess DT, Matsumoto A, Kim SO, Marshall HE, Stamler JS. Protein Snitrosylation: purview and parameters. Nat. Rev. Mol. Cell. Biol 2005;6:150–166. [PubMed: 15688001]
2. Hara MR, Snyder SH. Nitric oxide-GAPDH-Siah: a novel cell death cascade. Cell. Mol. Neurobiol 2006;26:527–538. [PubMed: 16633896]
3. Nakamura T, Lipton SA. Emerging roles of S-nitrosylation in protein misfolding and neurodegenerative diseases. Antioxid. Redox. Signal 2008;10:87–101. [PubMed: 17961071]
4. Gu Z, Kaul M, Yan B, Kridel SJ, Cui J, Strongin A, Smith JW, Liddington RC, Lipton SA. S-nitrosylation of matrix metalloproteinases: signaling pathway to neuronal cell death. Science 2002;297 (5584):1186–1190. [PubMed: 12183632]
5. Haendeler J, Hoffmann J, Tischler V, Berk BC, Zeiher AM, Dimmeler S. Redox regulatory and anti-apoptotic functions of thioredoxin depend on S-nitrosylation at cysteine 69. Nat. Cell. Biol 2002;4 (10):743–749. [PubMed: 12244325]
6. Xu L, Eu JP, Meissner G, Stamler JS. Activation of the cardiac calcium release channel (ryanodine receptor) by poly-S-nitrosylation. Science 1998;279(5348):234–237. [PubMed: 9422697]
7. Yoshida T, Inoue R, Morii T, Takahashi N, Yamamoto S, Hara Y, Tominaga M, Shimizu S, Sato Y, Mori Y. Nitric oxide activates TRP channels by cysteine Snitrosylation. Nat. Chem. Biol 2006;2(11): 596–607. [PubMed: 16998480]
8. Kharitonov VG, Sundquist AR, Sharma VS. Kinetics of nitrosation of thiols by nitric oxide in the presence of oxygen. J. Biol. Chem 1995;270(47):28158–28164. [PubMed: 7499306]
9. Wink DA, Nims RW, Darbyshire JF, Christodoulou D, Hanbauer I, Cox GW, Laval F, Laval J, Cook JA, Krishna MC, DeGraff WG, Mitchell JB. Reaction kinetics for nitrosation of cysteine and glutathione in aerobic nitric oxide solutions at neutral pH. Insights into the fate and physiological effects of intermediates generated in the NO/O2 reaction. Chem. Res. Toxicol 1994;7(4):519–525. [PubMed: 7981416]
10. Jourd'heuil D, Jourd'heuil FL, Feelisch M. Oxidation and nitrosation of thiols at low micromolar exposure to nitric oxide. Evidence for a free radical mechanism. J. Biol. Chem 2003;278(18):15720–15726. [PubMed: 12595536]
11. Keshive M, Singh S, Wishnok JS, Tannenbaum SR, Deen WM. Kinetics of Snitrosation of thiols in nitric oxide solutions. Chem. Res. Toxicol 1996;9(6):988–993. [PubMed: 8870986]
12. Möller M, Botti H, Batthyany C, Rubbo H, Radi R, Denicola A. Direct measurement of nitric oxide and oxygen partitioning into liposomes and low density lipoprotein. J. Biol. Chem 2005;280(10): 8850–8854. [PubMed: 15632138]
13. Subczynski WK, Wisniewska A, Yin JJ, Hyde JS, Kusumi A. Hydrophobic barriers of lipid bilayer membranes formed by reduction of water penetration by alkyl chain unsaturation and cholesterol. Biochemistry 1994;33(24):7670–7681. [PubMed: 8011634]

14. Liu X, Miller MJ, Joshi MS, Thomas DD, Lancaster JR Jr. Accelerated reaction of nitric oxide with O2 within the hydrophobic interior of biological membranes. Proc. Natl. Acad. Sci. USA 1998;95 (5):2175–2179. [PubMed: 9482858]
15. Möller MN, Li Q, Vitturi DA, Robinson JM, Lancaster JR Jr. Denicola A. Membrane “lens” effect: focusing the formation of reactive nitrogen oxides from the *NO/O2 reaction. Chem. Res. Toxicol 2007;20(4):709–714. [PubMed: 17388608]
16. Nedospasov A, Rafikov R, Beda N, Nudler E. An autocatalytic mechanism of protein nitrosylation. Proc. Natl. Acad. Sci. USA 2000;97(25):13543–13548. [PubMed: 11095728]
17. Zhang H, Bhargava K, Keszler A, Feix J, Hogg N, Joseph J, Kalyanaraman B. Transmembrane nitration of hydrophobic tyrosyl peptides – localization, characterization, mechanism of nitration and biological implications. J. Biol. Chem 2003;278:8969–8978. [PubMed: 12519728]
18. Frank S, Stallmeyer B, Kampfer H, Schaffner C, Pfeilschifter J. Differential regulation of vascular endothelial growth factor and its receptor fms-like-tyrosine kinase is mediated by nitric oxide in rat renal mesangial cells. Biochem. J 1999;338:367–374. [PubMed: 10024512]
19. Tarpey MM, Wink DA, Grisham MB. Methods for detection of reactive metabolites of oxygen and nitrogen: in vitro and in vivo considerations. Am. J. Physiol. Regul. Integr. Comp. Physiol 2004;286:R431–R444. [PubMed: 14761864]
20. Subczynski WK, Lomnicka M, Hyde JS. Permeability of nitric oxide through lipid bilayer membranes. Free Radic. Res. Commun 1996;24:343–349.
21. Altenbach C, Greenhalgh DA, Khorana HG, Hubbell WL. A collision gradient method to determine the immersion depth of nitroxides in lipid bilayers: application to spin-labeled mutants of bacteriorhodopsin. Proc. Nat. Acad. Sci 1994;91:1667–1671. [PubMed: 8127863]
22. Klug CS, Su W, Feix JB. Mapping of the residues involved in a proposed β-strand located in the ferric enterobactin receptor FepA using site-directed spin labeling. Biochemistry 1997;36:13027–13033. [PubMed: 9335564]
23. Nielsen RD, Che K, Gelb MH, Robinson BH. A ruler for determining the position of proteins in membranes. J. Am. Chem. Soc 2005;127(17):6430–6442. [PubMed: 15853351]
24. Keefer LK, Nims RW, Davies KM, Wink DA. “NONOates” (1-substituted diazen-1-ium-1,2-diolates) as nitric oxide donors: convenient nitric oxide dosage forms. Methods Enzymol 1996;268:281–293. [PubMed: 8782594]
25. Goss SPA, Singh RJ, Hogg N, Kalyanaraman B. Reactions of .NO, .NO_2 and peroxynitrite in membranes: physiological implications. Free Radic. Res 1999;31:597–606. [PubMed: 10630683]
26. McArthur PH, Shiva S, Gladwin MT. Measurement of circulating nitrite and Snitrosothiols by reductive chemiluminescence. J. Chromatogr. B Analyt. Technol. Biomed. Life Sci 2007;851:93–105.
27. Wang X, Bryan NS, MacArthur PH, Rodriguez J, Gladwin MT, Feelisch M. Measurement of nitric oxide levels in the red cell: validation of tri-iodide-based chemiluminescence with acid-sulfanilamide pretreatment. J. Biol. Chem 2006;281:26994–27002. [PubMed: 16845122]
28. Rhee KY, Erdjument-Bromage H, Tempst P, Nathan CF. S-nitroso proteome of *Mycobacterium tuberculosis*: Enzymes of intermediary metabolism and antioxidant defense. Proc. Natl. Acad. Sci. USA 2005;102:467–472. [PubMed: 15626759]
29. Erwin PA, Mitchell DA, Sartoretto J, Marletta MA, Michel T. Subcellular targeting and differential S-nitrosylation of endothelial nitric-oxide synthase. J. Biol. Chem 2006;281:151–157. [PubMed: 16286475]
30. Erilov DA, Bartucci R, Guzzi R, Shubin AA, Maryasov AG, Marsh D, Dzuba SA, Sportelli L. Water concentration profiles in membranes measured by ESEEM of spin-labeled lipids. J. Phys. Chem. B 2005;109(24):12003–12013. [PubMed: 16852481]
31. Subczynski WK, Widomska J, Feix JB. Physical properties of lipid bilayers from EPR spin labeling and their influence on chemical reactions in a membrane environment. Free Radic. Biol. Med 2009;46:707–18. [PubMed: 19111611]
32. Hess DT, Matsumoto A, Kim S-O, Marshall HE, Stamler JS. Protein Snitrosylation: Purview and parameters. Nat. Rev. Mol. Cell. Biol 2005;6:150–166. [PubMed: 15688001]

33. Ascenzi P, Colasanti M, Persichini T, Muolo M, Polticelli F, Venturini G, Bordo G, Bolognesi M. Re-evaluation of amino acid sequence and structural consensus rules of cysteine-nitric oxide reactivity. Biol. Chem 2000;381:623–627. [PubMed: 10987371]

34. Yao D, Gu Z, Nakamura T, Shi ZQ, Ma Y, Gaston B, Palmer LA, Rockenstein EM, Zhang Z, Masliah E, Uehara T, Lipton SA. Nitrosative stress linked to sporadic Parkinson's disease: S-nitrosylation of parkin regulates its E3 ubiquitin ligase activity. Proc. Natl. Acad. Sci. USA 2004;101(29):10810–10814. [PubMed: 15252205]

35. Chung KK, Thomas B, Li X, Pletnikova O, Troncoso JC, Marsh L, Dawson VL, Dawson TM. S-nitrosylation of parkin regulates ubiquitination and compromises parkin's protective function. Science 2004;304(5675):1328–1331. [PubMed: 15105460]

36. Zhang H, Xu Y, Joseph J, Kalyanaraman B. Influence of intramolecular electron transfer mechanism in biological nitration, nitrosation, and oxidation of redox-sensitive amino acids. Methods Enzymol 2008;440:65–94. [PubMed: 18423211]

37. Möller MN, Lancaster JR Jr. Denicola A. Acceleration of nitric oxide autoxidation and nitrosation by membranes. IUBMB Life 2007;59:243–248. [PubMed: 17505960]

38. Schoneich C, Sharov V. Mass spectrometry of protein modifications by reactive oxygen and nitrogen species. Free Radic. Biol. Med 2006;41:1507–1520. [PubMed: 17045919]

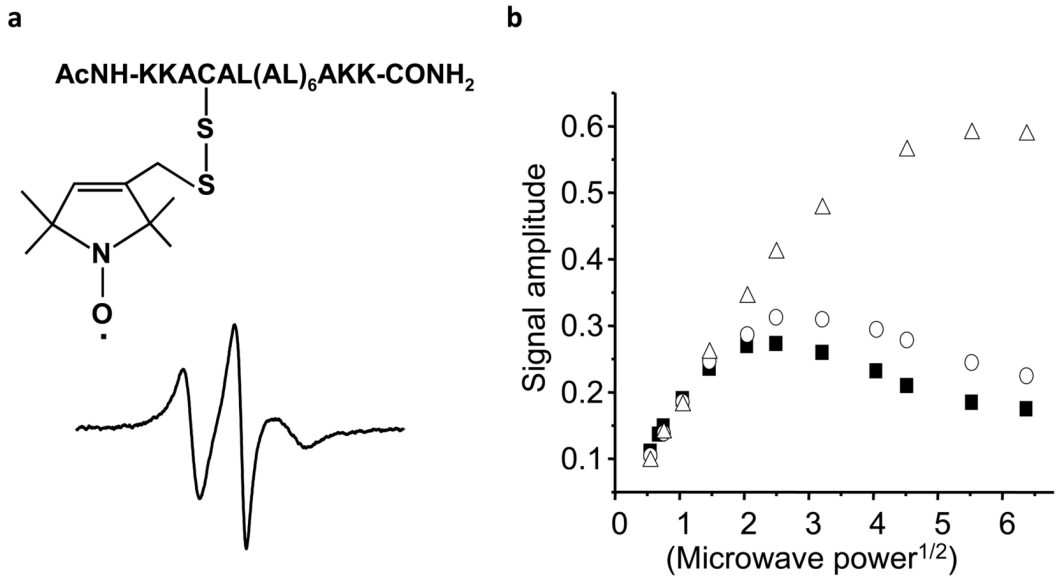

Figure 1. EPR spectrum of MTSL-labeled C_4 peptide in DLPC liposomes.

(a) The steady state EPR spectrum of MTSL-labeled C_4 (300 μM) in DLPC liposomes (30 mM). EPR parameters: Scan width, 100 G; modulation amplitude, 1 G; microwave power, 1 mW; scan time, 4 min. **(b)** The continuous wave microwave power saturation behavior of C_4 peptide in DLPC liposomes. Spectral data obtained under nitrogen (closed squares), air (open triangles), and under nitrogen in the presence of 100 mM NiEDDA (open circles).

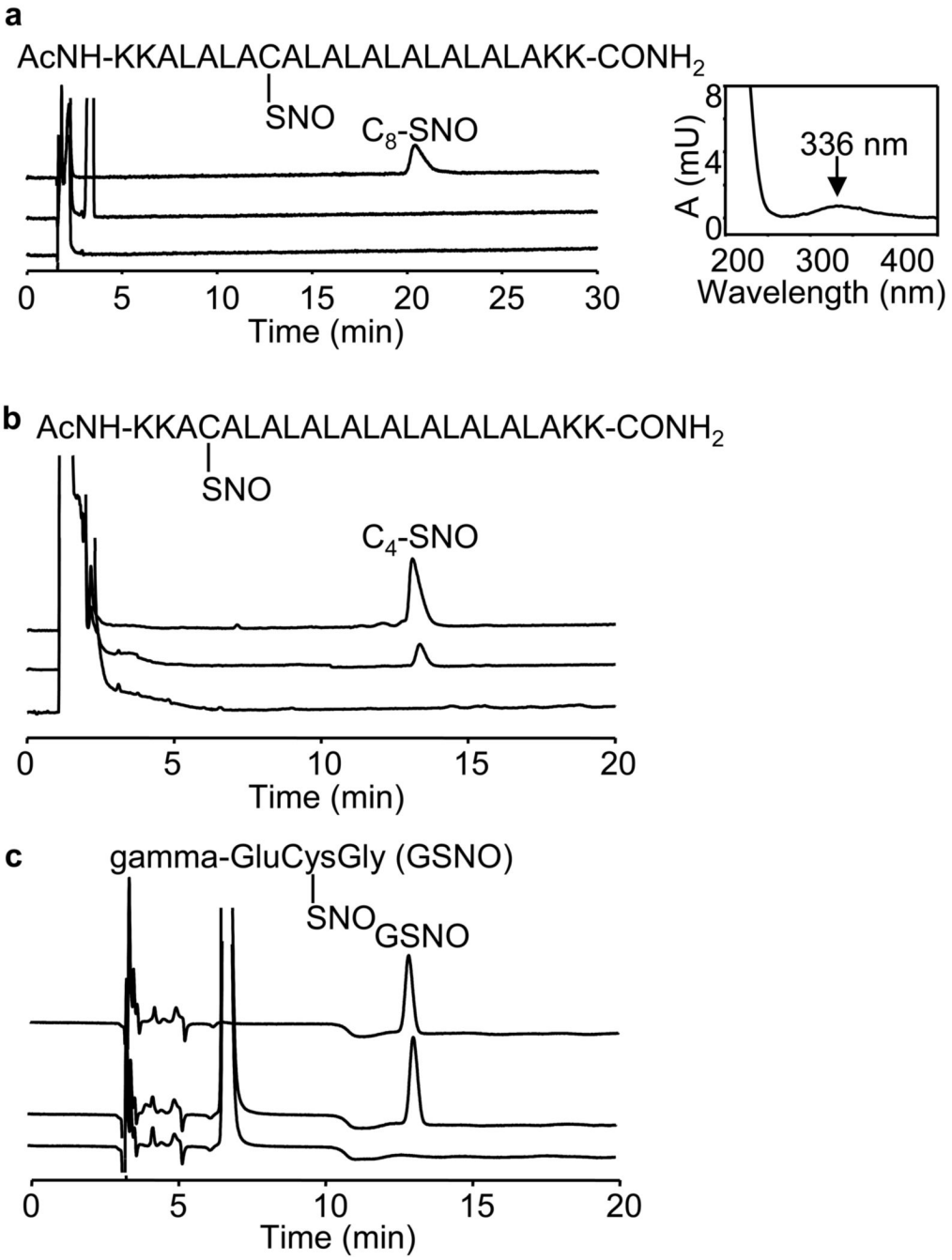

Figure 2. HPLC analyses of ˙NO-mediated S-nitrosation of GSH in aqueous buffer and transmembrane thiols, C_4 and C_8, in liposomes

(a) (*Top trace*) Authentic C_8-SNO (100 pmoles) was separated and detected at 336 nm. The peak eluted at 21 min. (*Middle trace*) C_8 peptide (300 μM) in DLPC liposome (30 mM) was incubated with DEA-NONOate (250 μM) for 20 min in a phosphate buffer (100 mM, pH 7.5) containing DTPA (100 μM). Iodoacetamide (50 mM) was added to the reaction mixture to block free thiols (after dissolving in methanol; 1:1 v/v). HPLC analysis was performed at 336 nm. (*Bottom trace*) same as above but without DEA-NONOate. **(b)** (*Top trace*) Authentic C_4-SNO (20 pmoles) was separated and detected at 336 nm. The peak eluted at 13.5 min. (*Middle trace*) same as *middle trace* in **(a)** except that C_4 peptide (300 μM) was used. (*Bottom trace*)

same as above but without DEA-NONOate. (*Inset*) The UV spectrum of a typical S-nitrosothiol (e.g., C_4-SNO) showed an absorption maximum at 336 nm. **(c)** (*Top trace*) Authentic GSNO was separated and detected at 336 nm. (*Middle trace*) Same as middle trace in **(b)** except that GSH (300 μM) was used. (*Bottom trace*) same as middle trace, above, but without DEA-NONOate.

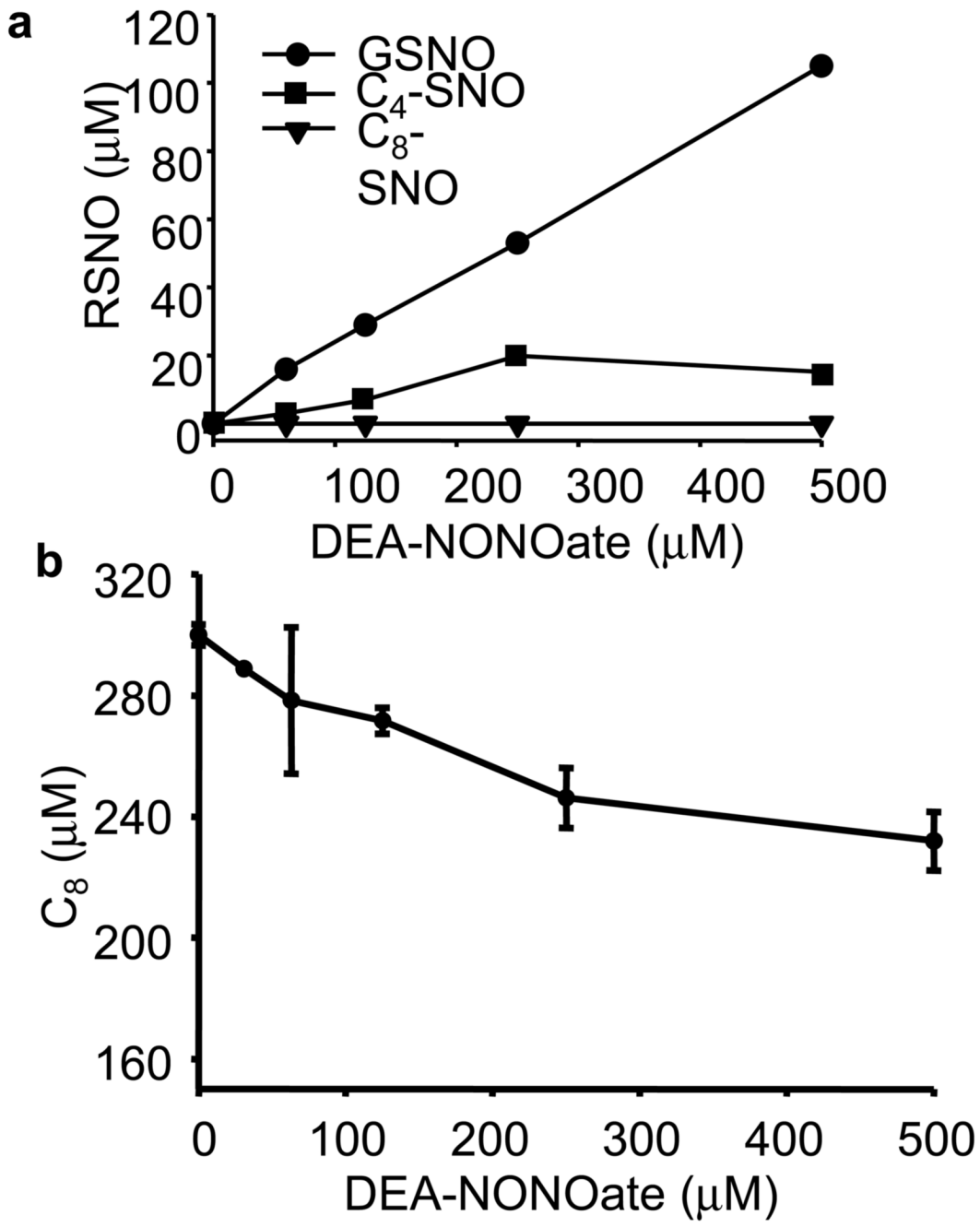

Figure 3. Formation of GSNO, C_4-SNO, and C_8-SNO and depletion of C_8 during $^{\cdot}$NO-mediated reactions of thiols

(**a)** GSH (300 μM) or C_4 (300 μM), and C_8 (300 μM) in DLPC liposomes were incubated in phosphate buffer (50 mM, pH 7.5) with various concentrations of DEA-NONOate as indicated for 30 min at 37° C, and the liposomes dissolved in methanol and analyzed by HPLC at 336 nm. The concentrations were determined using the authentic standards. **(b)** Experimental conditions were the same as in **(a)** for C_8 and analyzed by HPLC at 210 nm.

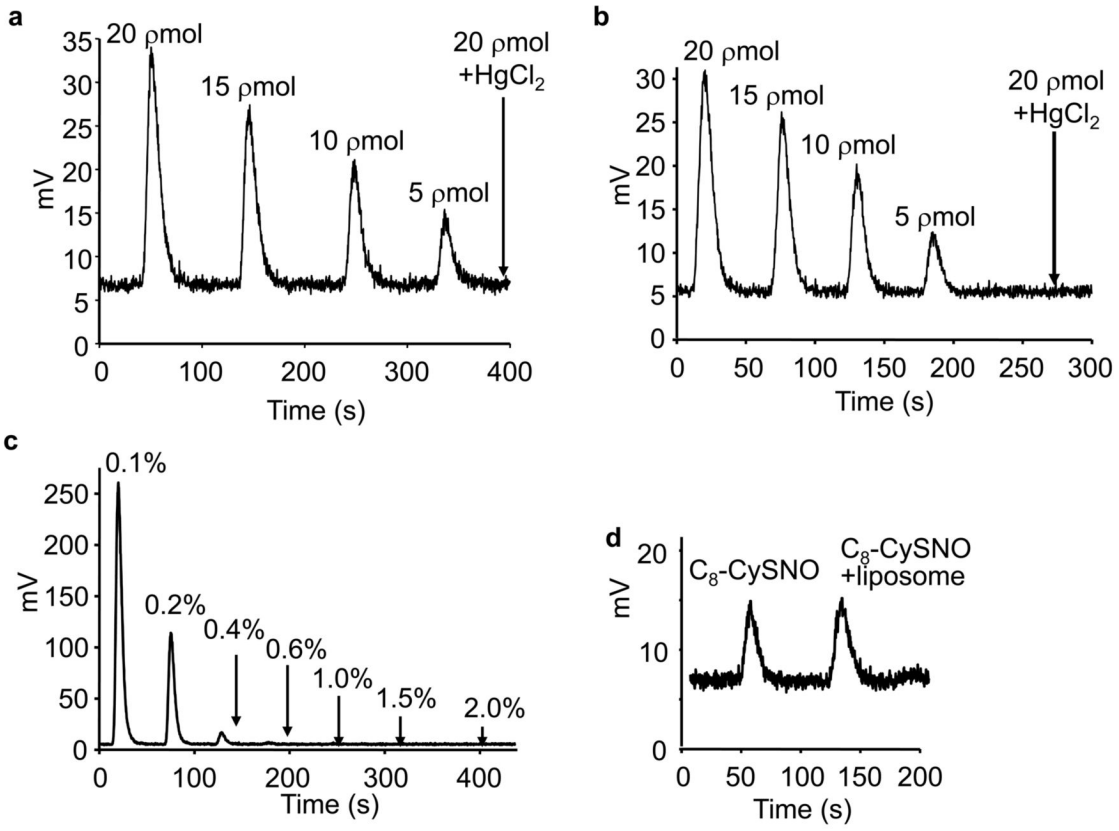

Figure 4. Tri-iodide chemiluminescence analyses of S-nitrosothiol standards

(a) Authentic GSNO (5-20 pmoles) was injected into a purge vessel containing 5 ml reaction solution [5.6 mg/ml potassium iodide and 3.6 mg/ml iodine in 77% acetic acid (v/v)]. Signals were detected in a Sievers Model 280A ·NO analyzer and recorded with Liquid software. Arrow indicates the effect of adding $HgCl_2$ to GSNO prior to injecting into the ·NO analyzer. **(b)** Same as **(a)** except that C_8-SNO (5-20 pmoles) was used. Arrow indicates the signal in response to pretreatment of C_8-SNO in a methanolic solution with $HgCl_2$. **(c)** Nitrite anion (200 pmoles) was added to DLPC liposome (30 mM) in a phosphate buffer (50 mM, pH 7.5) containing DTPA (100 μM). Samples (100 μl) were mixed with 10 μl of 2H HCl and various amounts of ammonium sulfamide and incubated for 15 min in ice. Aliquots were then injected into the ·NO analyzer. **(d)** Authentic C_8-SNO (5 pmoles) and C_8-SNO mixed with 30 mM DLPC liposomes was tested to investigate the interference of DLPC on C_8-SNO detection.

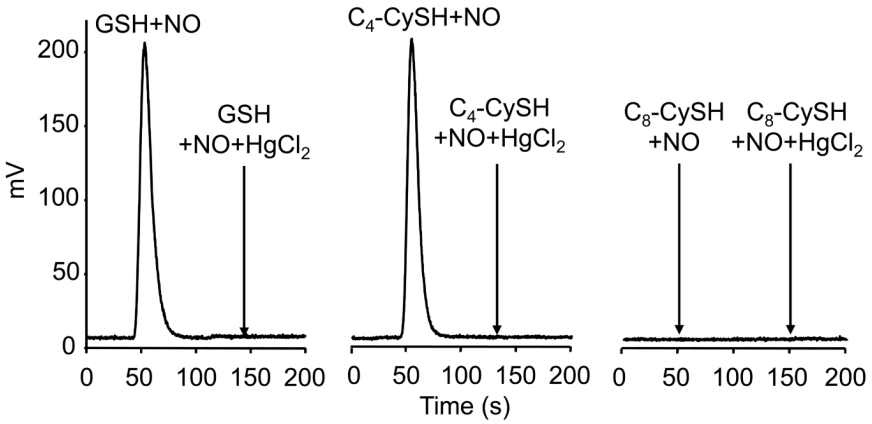

Figure 5. Tri-iodide chemiluminescence analysis of ˙NO-mediated S-nitrosation of GSH in aqueous buffer and transmembrane thiols, C_4 and C_8, in liposomes

C_4 and C_8 peptides (300 μM) in DLPC liposomes (30 mM) or GSH (300 μM) were incubated with 100 μM DEA-NONOate in a phosphate buffer (50 mM, pH 7.5) containing DTPA (100 μM) for 30 min. Iodoacetamide (50 mM) was added to the liposomal reaction mixtures dissolved in methanol. Samples were subsequently analyzed in an ˙NO analyzer. (*Left*) Signals were obtained from injecting 10 μl of reaction mixtures containing GSH. Arrow indicates the change in signal intensity in response to pretreatment with $HgCl_2$ (5 mM). (*Middle*) same as (*left*) except that 100 μl of reaction mixtures containing C_4 peptide was injected. Arrow indicates the effect of $HgCl_2$. (*Right*) same as (*middle*) except that 100 μl of reaction mixtures containing C_8 peptide was injected.

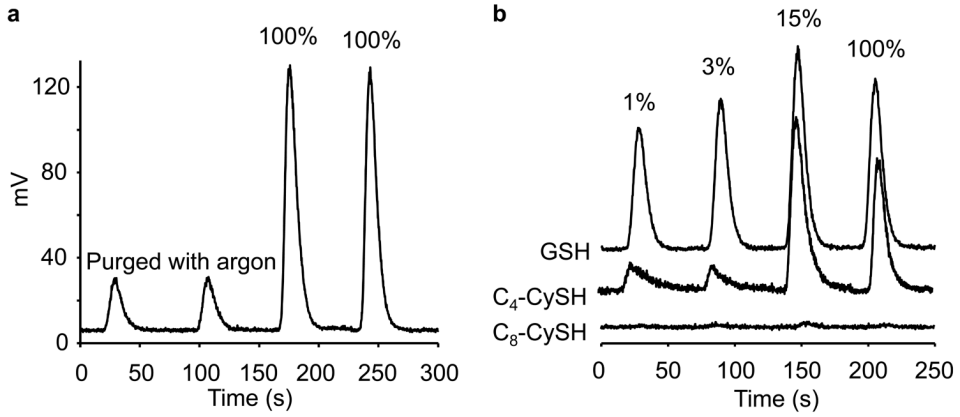

Figure 6. The influence of oxygen concentration on ·NO-mediated S-nitrosation of transmembrane hydrophobic thiols, C_4 and C_8, and GSH

Experimental conditions were the same as described in Figure 2. Experiments were performed in an oxygen-free glove box, and indicated aerobic levels were achieved by purging the glove box with appropriate air and argon mixture. Oxygen-depleted reagents were prepared by degassing with argon. (**a**) GSH (300 μM) in phosphate buffer (50 mM, pH 7.5) was incubated with DEA-NONOate in 100% air or in argon for 30 min. The actual traces obtained under argon-purged conditions and 100% air-saturation are shown in duplicate. The residual signal obtained in argon is attributed to air contamination. (**b**) Signals were obtained from incubations containing 300 μl of GSH, C_4, and C_8 and DEA-NONOate (50 μM) in DLPC liposome (30 μM) and phosphate buffer (50 mM) containing DTPA (100 μM) for 30 min at indicated aerobic levels. Data shown are representative of four independent experiments.

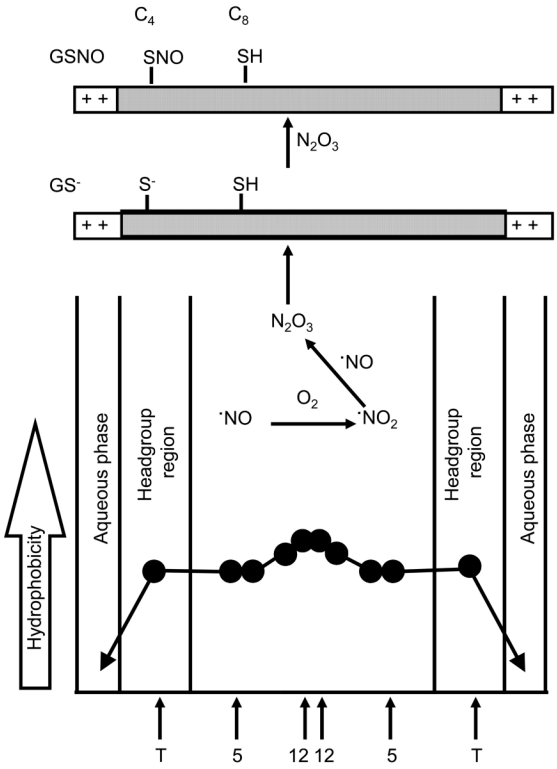

Figure 7. S-nitrosation of transmembrane peptides in membranes as a function of hydrophobicity
Approximate locations of the nitroxide moieties of stearic acid spin labels are indicated by arrows.